



Extended summary

Nonlinear dynamics in microelectromechanical systems

Curriculum: Architecture, Buildings and Structures

Author

Laura Ruzziconi

Tutor

Stefano Lenci

Cotutor

Mohammad I. Younis

Date: 31-10-2010

Abstract. This study is suggested by the growing attention, both from a practical and a theoretical point of view, toward the nonlinear behaviour of microelectromechanical systems (MEMS). The dissertation considers two different case-studies.

In the first case-study, the nonlinear dynamics of a MEMS device subjected to a constant axial load, electrostatically and electro-dynamically actuated and with a very shallow arched initial shape simulating the imperfections due to the microfabrication process are analyzed. The aim is that of illustrating the nonlinear phenomena which arise due to the coupling of mechanical and electrical nonlinearities and discussing their usefulness for the engineering design of the microstructure. An accurate single degree of freedom reduced-order model is derived. The device is investigated in a neighbourhood of the bifurcation from a single to a double potential well. Systematic numerical simulations are performed by the combined use of frequency response diagram, behaviour chart, attractor-basins phase portraits. The main features of the nonlinear dynamics are investigated in detail, as the non-resonant and resonant oscillations with softening behaviour, the coexistence of several robust attractors leading to a considerable versatility of behaviour, the safe basin erosion.

In the second case-study, starting from the experimental data of dynamic pull-in due to a frequency-sweeping process in a capacitive accelerometer, a dynamical integrity analysis is performed. The loss of dynamical integrity is investigated by curves of constant percentage of integrity factor. It is found that these curves follow exactly the experimental data and succeed in



Doctoral School on Engineering Sciences

Università Politecnica delle Marche

interpreting the existence of disturbances. The theoretical curves of disappearance of the attractors, instead, represent the limit when disturbances are absent, which never occurs in practice. Also, the obtained behaviour chart can serve as a design guideline in order to ensure safety of the device.

Keywords. Dynamical integrity, integrity factor, microelectromechanical systems, nonlinear dynamics, reduced-order models.

1 Problem statement and objectives

The first case-study is suggested by the growing attention toward MEMS devices showing nonlinear dynamical phenomena in their response. Recently, many works emphasize the possibility to utilize them in a lot of kinds of applications and they remark the importance of modeling the nonlinear behavior of the device in order to capture the full dynamic picture of its response.

For instance, Nayfeh *et al.* [1] consider an electrically actuated straight microbeam and explore its nonlinear static and dynamic response. They provide an analytical formulation of a reduced-order model derived by the classical Galerkin technique. Gottlieb and Champneys [2] analyze a nonlinear thermoelastic microbeam electrically actuated. They estimate the threshold that triggers the erosion phenomenon leading to dynamic pull-in by determining the homoclinic bifurcation with the Melnikov method. Lenci and Rega [3] further develop this analysis focusing on the erosion of the basins and the loss of dynamical integrity. They employ the results to design a controller based on shifting the homoclinic bifurcation to higher excitation amplitudes. Krylov and Dick [4] make a careful potential wells analysis in order to investigate the nonlinear dynamic response of initially curved shallow microbeams. Their study is motivated by the possibility of interesting applications due to the static bistability of the device. Ouakad and Younis [5] studied the dynamics of MEMS arches under electric harmonic excitation using a shooting technique and the Floquet theory. Abu-Salih and Elata [6] investigate theoretically and experimentally buckling of clamped-clamped microbeam with an axial force induced through electrostatic actuation at its edge.

This work deals with the MEMS device in Figure 1. It is made of a fixed-fixed microbeam subjected to a constant axial load. It is electrostatically and electrodynamically actuated. The imperfections due to the microfabrication process are simulated by modeling the imperfect beam as a very shallow arch with small initial rise. Contrary to other studies where only a small axial load is taken into account to simulate residual stresses, in this work an elevated value of axial load is considered in order to analyze the device in a neighborhood of the bifurcation from a single to a double potential well. The aim is to examine the nonlinear dynamic phenomena of its response and to focus on the related potential applications.

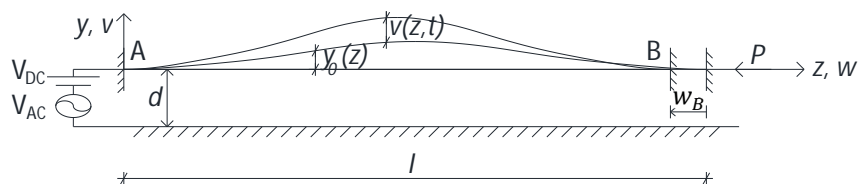


Figure 1. A schematic of the MEMS device.

The second case-study deals with the interpretation of experimental pull-in data using the dynamical integrity analysis. In fact, as remarked by Thompson [7], the existence of an attractor in a dynamical system does not guarantee its safety from a practical point of view. This is because in experiments and practice, disturbances exist, giving uncertainty to the

operating initial conditions. If the safe basin is not sufficiently robust, the dynamical outcome can be totally different from what is theoretically predicted. In MEMS devices, it may produce the escape, which manifests itself through the dynamic pull-in, i.e. the resonating microstructure collapses on the substrate leading to its failure through stiction or short circuiting [8].

This work starts from the experimental data of dynamic pull-in of a particular MEMS device, the capacitive accelerometer shown in Figure 2. The data are obtained in [9] by a frequency-sweeping process, where the voltage is kept fixed and the frequency is increased or decreased slowly, i.e. quasi-statically. The main theoretical motivation is to highlight the effectiveness of the dynamical integrity analysis for interpreting the experimental data. In particular, the curves of constant percentage of integrity factor are constructed and it is shown that they follow exactly the experimental data, succeeding in the interpretation of the presence of disturbances.

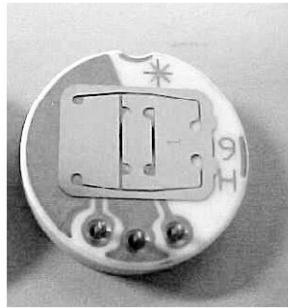


Figure 2. A picture of the capacitive accelerometer.

2 Research planning and activities

In the first case-study, the MEMS device in Figure 1 is analyzed using a mechanical model which includes geometric nonlinearities as well as nonlinearities due to the electric force. The microbeam is modeled according to the Euler-Bernoulli theory, and a linearly elastic isotropic and homogeneous material is assumed. The axial displacement is condensed by a classical procedure [10]. After the nondimensionalization, the mechanical behavior of the device is described by the nonlinear PDE

$$\begin{aligned} & \ddot{v}(z,t) + \xi \dot{v}(z,t) + v''''(z,t) + \alpha(v''(z,t) + y_0''(z)) \\ & = -\gamma \frac{(V_{DC} + V_{AC} \cos(\Omega t))^2}{(1 + v(z,t) + y_0(z))^2} \end{aligned} \quad (1)$$

with

$$\alpha = n - ka I_1 \quad I_1 = \int_0^1 \left(\frac{1}{2} (v'(z,t))^2 + v'(z,t) y_0'(z) \right) dz \quad (2)$$

where the boundary conditions are

$$v(0,t) = 0, \quad v(1,t) = 0, \quad v'(0,t) = 0, \quad v'(1,t) = 0. \quad (3)$$

It is referred to a realistic case, where the thickness of the microbeam is $1.4 \mu\text{m}$ (micron), the width is $25 \mu\text{m}$, the length is $400 \mu\text{m}$, the arched shape is $y_0(z) = y_0(1 - \cos(2\pi z))/2$, the maximum initial rise is $y_0 = 0.01 \mu\text{m}$. The gap d is $1.7 \mu\text{m}$, the electrostatic voltage is $V_{DC} = 0.8 \text{ V}$, the damping coefficient is 0.0002 Ns/m and the axial load is $n = 41$ and $n = 43$, respectively, for the case of a single and of a double potential well. The two different behaviors are analyzed and compared. In the following it is referred to the double-well case, which is particularly interesting.

The static and the linear dynamics are analyzed and their results are used to generate a reduced-order model of the nonlinear dynamics.

The static equation cannot be solved in closed form, because of the electric term. It is investigated using a single degree of freedom (d.o.f.) Galerkin reduced-order model [11], where the basis function is derived from a simplified nonlinear model (obtained from the static equation by approximating the electric term with its zero order Taylor expansion) which can be analytically solved.

The linear dynamic analysis [12, 13] is performed and the first four eigenvalues and the first four orthonormal mode shapes are obtained, both in the case of linear motion around the unstable equilibrium (the first eigenvalue is negative since the analysis refers to the unstable configuration) and in the case of linear oscillations around the lower and the upper stable configuration. It can be noticed that there are no 1:1, 2:1 and 3:1 internal resonances.

In order to have a good representation of the nonlinear dynamics of the device, it's worth noting that, because of the nonlinearities, the reduced-order model requires a careful modeling, especially of the potential wells, both at the equilibria and, remarkably, at the transition to the escape. This is crucial, since the system response is investigated up to high values of electrodynamic voltage. A single d.o.f. Galerkin reduced-order model of the nonlinear dynamics is derived projecting the dynamics on the eigenfunctions around the nonlinear unstable static configuration. This choice produces a slight approximation in both wells, without causing large errors. This is appropriate for the purposes of this work, since it focuses on the global behavior in both the wells, and not only on the response in one particular well. Moreover, other reduced-order models are considered and compared.

In the second case-study, the response of the device is simulated by a nonlinear single d.o.f. model, where the parameters are obtained from experimental measurements and tests. It shares the same main qualitative features of other softening systems investigated in depth [2, 3]. From the classical nonlinear dynamical analysis it can be noticed that the theoretical pull-in (inevitable escape), bounded by the saddle-node (SN) bifurcation and the boundary crisis (BC), is systematically above the experimental pull-in threshold, as can be seen in the forthcoming Figure 5. Hence, identifying the inevitable escape zones does not succeed in predicting the experimental pull-in bands. This calls for a more detailed analysis, where also dynamical integrity concepts are considered.

It is focus on the range where the tongues of the escape enter the potential well. Examples of this are represented in Figures 3.

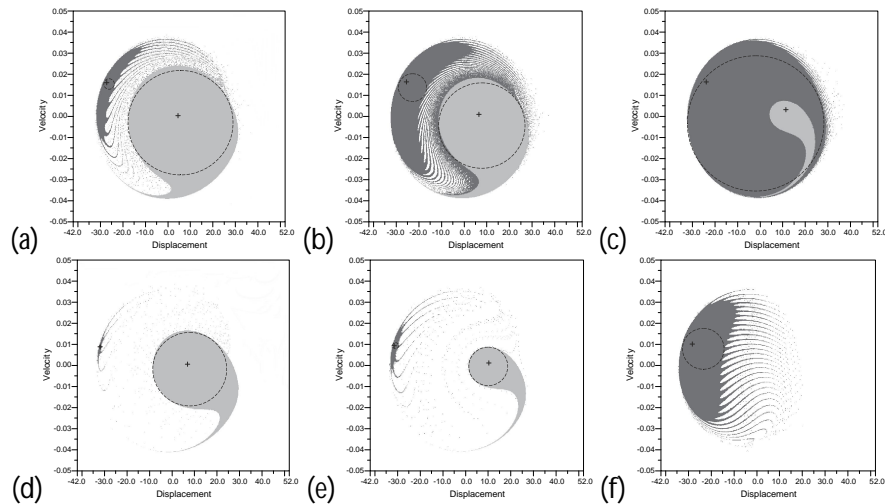


Figure 3. Attractor-basins phase portraits for $V_{AC} = 8$ V and (a) $\Omega = 180$ Hz, (b) $\Omega = 183$ Hz, (c) $\Omega = 185$ Hz; $V_{AC} = 15$ V and (d) $\Omega = 178$ Hz, (e) $\Omega = 181$ Hz, (f) $\Omega = 187$ Hz. The circles used in the definition of the IF are in dashed lines.

The escape separates the basins of attraction of the resonant and non-resonant attractor preventing the safe jump between them (although they coexist) and produces the shrinkage and the erosion of the safe basins up to their complete destruction for sufficiently high dynamic voltage.

3 Analysis and discussion of main results

In the first case study, the single d.o.f. reduced-order model previously obtained is investigated performing a nonlinear dynamical analysis. The numerical simulations are conducted according to the guideline of the classical studies in [14-17].

In a neighborhood of the resonance, the device behaves similarly to a softening oscillator. To distinguish between the attractors belonging to the rest potential well and to the other well, in the following they are named, respectively, A and B. All the couples of non-resonant and resonant oscillation show the characteristic bending toward the left in the frequency response curve.

Several frequency response curves are obtained for different values of the applied voltage V_{AC} . They permit to draw the behavior chart in Figure 4 which has the typical softening characteristics [3]: the Δ -shaped region of coexistence of the resonant and the non-resonant attractor, the V-shaped region where the two attractors do not exist and the cusp where the saddle-node bifurcations of the two attractors collapse.

These numerical simulations show that the device has a considerable versatility of behavior, due to the coexistence of several attractors. This is an uncommon phenomenon in traditional MEMS [9]. It can be used in different kinds of applications. For instance, the device can switch from an oscillation to another one, by simply modifying the initial conditions, which may be desirable in detection applications. These results allow identifying the most suitable ranges to operate the device according to the desired outcome.

All the results for the case of a double potential well are compared to those of the single d.o.f. dynamics for the case of a single potential well.

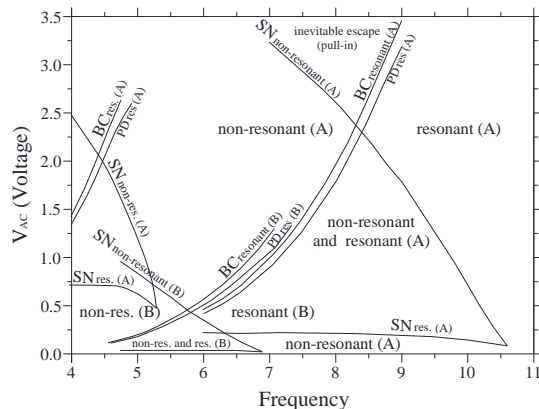


Figure 4. Behavior chart of the main bifurcations.

In the second case-study, the dynamical integrity analysis is performed. A continuous parallelism between theory and experiments is established. All the chosen theoretical tools are constantly justified by the experimental conditions of the sweeping process.

Since we are interested in the vibrations of the device at steady state, following previous studies [3, 18], the safe basin is considered as the union of the classical basins of attraction of all the attractors inside the potential well, i.e. the union of the basins of the non-resonant and resonant attractor.

The integrity factor (IF) introduced in [19] is chosen as a measure of the dynamical integrity of the safe basin. The IF is the normalized radius of the largest circle entirely belonging to the safe basin. It is an appropriate measure for the considered case-study. In fact, it is a property of the safe basin and not of the attractor. It focuses on the compact 'core' of the safe basin, ruling out the fractality that induces unpredictability of motion. Finally, it is computed in the steady dynamics, neglecting the transient, which is suitable for these experimental data because they come from a sweeping process, where at the end of each step the system is in steady state conditions. Examples of the circles used in the definition of the IF are depicted in Figures 3a-f in dashed line.

Erosion profiles are drawn to investigate the loss of structural safety when the parameters are varying. They are obtained plotting the IF as a function of the increasing frequency amplitude. They describe the changes in the IF, which depend both on the increased fractality and on the shrinkage of the basins.

Several erosion profiles are made for different values of V_{AC} and the curves of constant percentage of IF are obtained and reported in the behavior chart in Figure 5. They summarize the overall scenario of the loss of structural integrity in the analyzed device. The experimental data follow "exactly" these curves. Below a certain percentage, the device becomes practically vulnerable to dynamical pull-in, since the safe basin is not sufficiently robust to tolerate the disturbances and the discontinuous steps coming from the sweeping process. Therefore, not only the classical area of inevitable escape, but also the practical pull-in area has to be avoided.

The chart has also a practical benefit. In fact, it serves as a guideline for the design. Depending on the expected disturbances, it allows to identify the most dangerous ranges in order that the safety of the device is ensured.

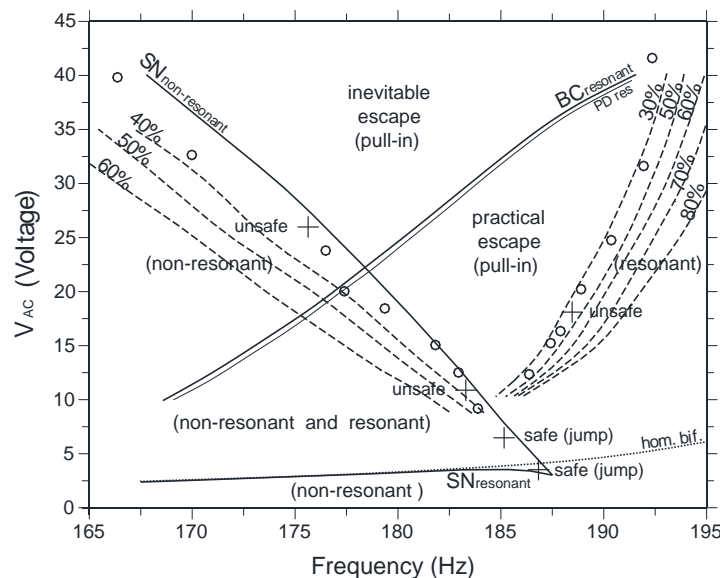


Figure 5. Frequency-dynamic voltage behavior chart. The solid lines correspond to the main dynamical phenomena in the attractors; the dotted line to the homoclinic bifurcation; the dashed lines to the curves of constant percentage of IF; the dots to the experimental data.

4 Conclusions

The dissertation has analyzed the nonlinear dynamic behavior in two case-studies of MEMS devices.

In the first case-study, the dynamical response of an electrostatically and electro-dynamically actuated MEMS device based on a slender imperfect microbeam subjected to an axial load of compression has been investigated. The device has been analyzed in a neighborhood of the bifurcation from a single to a double potential well, focusing, especially, on this last case. The issue of modeling the nonlinear behavior in order to capture the full dynamic picture of the mechanical system has been addressed. Systematic numerical simulations have been performed, using a single d.o.f. Galerkin reduced-order model. The behavior chart has been obtained, which represents the main features of the overall scenario of the nonlinear dynamic response. The coexistence of some robust attractors has been further examined both from a practical and a theoretical point of view using a basins of attraction analysis. The considerable versatility of behavior of the device has been highlighted. It is expected that more complicated models may further enrich the accuracy of the results, although this single d.o.f. reduced-order model, despite being very simple, is able to describe the main qualitative aspects of the nonlinear dynamics of the device.

In the second case-study, investigating the response of a capacitive accelerometer at primary resonance, the issue of the dynamical integrity in a mechanical system has been addressed. Its qualitative evaluation has been performed, choosing the most suitable tools according to the considered experimental conditions. The effectiveness of this analysis has been highlighted, showing the accuracy of the curves of constant percentage of IF in interpreting the existence of disturbances in experiments and practice. Also, their use in a design has been proposed.

References

- [1] Nayfeh, A. H., Younis, M. I., and Abdel-Rahman, E. M., 2007, "Dynamic pull-in phenomenon in MEMS resonators," *Nonlinear Dyn.*, **48**, pp. 153-163.
- [2] Gottlieb, O., and Champneys, A. R., 2005, "Global bifurcations of nonlinear thermoelastic microbeams subject to electrodynamic actuation," *IUTAM Symp. On Chaotic Dynamics and Control of System and Processes in Mechanics Solid Mechanics and Its applications*, ed. Rega G and Vestroni F, Berlin, Springer, **122**, pp. 47-57.
- [3] Lenci, S., and Rega, G., 2006, "Control of pull-in dynamics in a nonlinear thermoelastic electrically actuated microbeam," *J. Micromech. Microeng.*, **16**, pp. 390-401.
- [4] Krylov, S., and Dick, N., 2010, "Dynamic stability of electrostatically actuated initially curved shallow micro beams," *Continuum Mech. Thermodyn.*, **22**, pp. 445-468.
- [5] Ouakad, H. M., and Younis, M. I., 2010, "The dynamic behavior of MEMS arch resonators actuated electrically," *Int. J. Non-Linear Mech.*, **45**, pp. 704-713.
- [6] Abu-Salih, S., and Elata, D., 2006, "Experimental Validation of Electromechanical Buckling," *J. Microelectromech. Sys.*, **15**, pp. 1656-1662.
- [7] Thompson, J. M. T., 1989, "Chaotic behaviour triggering the escape from a potential well," *Proc. Roy. Soc. London A*, **421**, pp. 195-225.
- [8] Senturia, S. D., 2001, *Microsystem design*. Kluwer Academic Publishers, Dordrecht.
- [9] Alsaleem, F. M., Younis, M. I., and Ruzziconi, L., 2010, "An experimental and theoretical investigation of dynamic pull-in in MEMS resonators actuated electrostatically," *J. Microelectromech. Sys.*, **19**, pp. 794-806.
- [10] Villaggio, P., 1997, *Mathematical Models for Elastic Structures*, Cambridge University Press, Pisa.
- [11] Rega, G., and Troger, H., 2005, "Dimension Reduction of Dynamical Systems: Methods, Models, Applications," *Nonlinear Dyn.*, **41**, pp. 1-15.
- [12] Nayfeh, A. H., Kreider, W., and Anderson, T. J., 1995, "Investigation of Natural Frequencies and Mode Shapes of Buckled Beams," *AIAA Journal*, **33**(6), pp. 1121-1126.
- [13] Lacarbonara, W., and Rega, G., 2003, "Resonant non-linear normal modes. Part II: activation/orthogonality conditions for shallow structural systems," *Int. J. Non-Linear Mech.*, **38**, pp. 873-887.
- [14] Szemplinska-Stupnicka, W., 1992, "Cross-well chaos and escape phenomena in driven oscillators," *Nonlinear Dyn.*, **3**, pp. 225-243.
- [15] Rega, G., Salvatori, A., and Benedettini, F., 1995, "Numerical and geometrical analysis of bifurcation and chaos for an asymmetric elastic nonlinear oscillator," *Nonlinear Dyn.*, **7**, pp. 249-272.
- [16] Szemplinska-Stupnicka, W., and Tyrkiel, E., 2002, "Sequences of global bifurcations and the related outcomes after crisis of the resonant attractor in a nonlinear oscillator," *Int. J. Bif. Chaos*, **12**, pp. 159-168.
- [17] Guckenheimer, J., and Holmes, P. J., 1983, *Nonlinear Oscillations, Dynamical Systems and Bifurcations of Vector Fields*. Springer-Verlag, New York.
- [18] Rega, G., and Lenci, S., 2005, "Identifying, evaluating, and controlling dynamical integrity measures in nonlinear mechanical oscillators," *Nonlin. Anal. TM&A*, **63**, pp. 902-914.
- [19] Lenci, S., and Rega, G., 2003, "Optimal control of nonregular dynamics in a Duffing oscillator." *Nonlinear Dyn.*, vol. **33**, pp. 71-86.